Measurement of Heat Transfer in Unbonded Silica Fibrous Insulation and Comparison with Theory

Kamran Daryabeigi

George R. Cunnington

Jeffrey R. Knutson

ABSTRACT

Effective thermal conductivity of a high porosity unbonded silica fibrous insulation specimen was measured over a pressure range of 0.001 to 750 torr (0.1 to 101.3×10^3 Pa), and with large temperature gradients maintained across the sample thickness: hot side temperature range of 360 to 1360 K, with the cold side at room temperature. The measurements were compared with the theoretical solution of combined radiation/conduction heat transfer. The previously developed radiation heat transfer model used in this study is based on a modified diffusion approximation, and uses deterministic parameters that define the composition and morphology of the medium: distributions of fiber size and orientation, fiber volume fractions, and the spectral complex refractive index of the fibers. The close agreement between experimental and theoretical data further verifies the theoretical model over a wide range of temperatures and pressures.

INTRODUCTION

Heat transfer through fibrous insulations has been the subject of great interest in the aerospace community for many years because of their use in thermal protection systems (TPS) for moderate to high temperature applications. The fibrous insulation systems used are either in bonded or unbonded form. The unbonded form consists of loose fibrous insulation mats of fibers. The Space Shuttle Orbiter tiles are an example of bonded insulation, where the tile is manufactured by sintering silica fibrous insulation mats to obtain a rigid structure. The focus of this paper is on an unbonded silica fibrous insulation.

Heat transfer through these high-porosity insulations is composed of combined radiation/conduction heat transfer. The conduction consists of both solid and gaseous conduction. In fibrous insulations with densities of 20 kg/m^3 or higher, natural convection is insignificant [1, 2]. Solid conduction is the least significant

Kamran Daryabeigi, NASA Langley Research Center, MS 190, Hampton, VA 23681
George R. Cunnington, Cunnington and Associates, Palo Alto, CA 24061
Jeffrey R. Knutson, NASA Langley Research Center, MS 424, Hampton, VA 23681

component of heat transfer for high porosity unbonded fibrous insulations. Radiation is the dominant mode of heat transfer, with its significance increasing with increasing temperature, while the contribution of gas conduction is dependent on the static pressure, being negligible in vacuum conditions and increasing with increasing static pressure.

Theoretical modeling of solid conduction through fibers and points of contact between them is difficult, therefore, various empirical and semi-empirical relations are used [3, 4]. Modeling of gas conduction in fibrous insulations requires knowledge of characteristic length (pore size), gas mean free path, and fiber orientation [3, 5]. Modeling of radiation heat transfer through fibrous insulations is more complicated, and has been the subject of various studies. A comprehensive review of various radiation models used for fibrous insulations is provided in Ref. [6].

The standard practice for modeling heat transfer through fibrous insulations uses thermal conductivity measurements as a function of temperature and pressure obtained using either steady-state [7] or transient [8] techniques. The measured thermal conductivity lumps the contributions of the various modes of heat transfer without providing any insight into the physics or the contribution of the various modes, therefore, in the present discussion it will be referred to as lumped thermal conductivity. The tabulated lumped thermal conductivity data are then used for analysis and design of TPS. One shortcoming of this technique is that the generated lumped thermal conductivity data are applicable only to the specific composition used, and if some of the composition parameters, such as density, change, a new set of data is needed. The use of lumped thermal conductivities in predicting surface or internal temperature response of ceramic tiles in transient tests with rapid surface heating has resulted in discrepancies between measured and predicted temperatures [7, 9, 10].

Significant work has been devoted to developing physics-based heat transfer modeling for bonded and unbonded fibrous insulations with various degrees of complexity. The simplest approach has been to use combined radiation/conduction heat transfer using a radiative thermal conductivity in terms of the Rosseland mean coefficient based on the diffusion approximation and assuming gray behavior and isotropic scattering [11, 12]. Later models used more refined radiation models based on scattering intensity distribution from infinite cylinders based on scattering solutions of Maxwell's equations [13, 14]. These more complex radiation models did not yield better agreement with experimental data, because they did not properly account for the two-dimensional scattering characteristics of fibers in the medium. Lee developed a rigorous formulation for scattering properties of fibrous insulations that accounted for the fiber orientation, with the radiative properties defined as a function of orientation, size distribution, and volume fraction of fibers [15, 16]. The resulting radiation model uses deterministic parameters that define the composition and morphology of the medium: distributions of fiber size and orientation, fiber volume fractions, and the spectral complex refractive index of the fibers. Lee and Cunnington used this radiative modeling in their combined radiation/conduction heat transfer analysis and compared their predictions with experimental data on bonded and unbonded fibrous insulation samples [4]. This

theory will be used in the present study to compare with experimental steady state data on an unbonded silica fibrous insulation.

Experimental data over a wide range of pressures and temperatures are needed for verification of radiation/conduction models developed by Lee and Cunnington [4]. Steady state thermal conductivity data are typically more suitable for this purpose. The guarded hot plate [17] is the standard technique for generating total thermal conductivity of fibrous insulation samples subject to small temperature gradients across the sample thickness. This technique is typically limited to a maximum temperature of 1255 K, and obtaining steady-state conditions may be cumbersome. A simplified steady state apparatus for measuring the effective thermal conductivity of highly porous samples subject to a large temperature gradient maintained across the sample thickness was used in the present study. The apparatus does not yield direct thermal conductivity as a function of temperature, but provides thermal conductivity integrated over a large temperature gradient, thus referred to as effective thermal conductivity. The measured effective thermal conductivity of a silica fibrous insulation sample, Q-fiber[*], over a wide range of temperatures and pressures was used for verification of the theoretical model [4]. This material is an efficient insulation that has previously been characterized both experimentally [18] and theoretically [4].

EXPERIMENTAL APPROACH

Steady state tests were conducted on a Q-fiber test sample in the NASA Langley Research Center's (LaRC) thermal-vacuum testing apparatus, described in detail elsewhere [19, 20]. The steady state test measures the effective thermal conductivity of a test sample with a large temperature difference maintained across the sample thickness, and follows the general guidelines of the American Society of Testing and Materials (ASTM) Standard C201 [21].
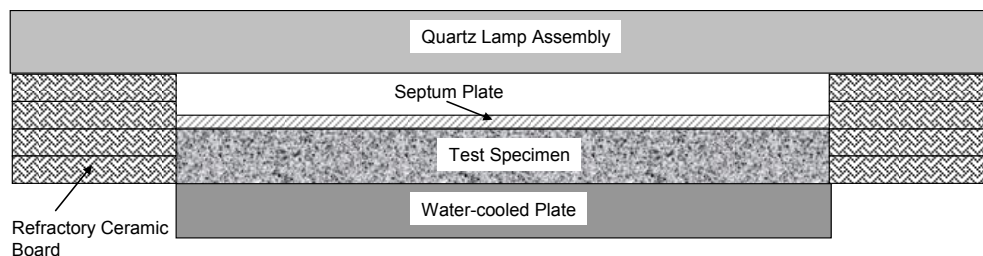

Figure 1. Schematic of steady state test setup

A schematic of the steady state test setup is shown in Figure 1. The main components of the setup are: a quartz lamp radiant heater array, an Inconel septum plate, a water cooled plate, test specimen, and refractory ceramic board insulation as shown in the figure. The water-cooled plate is equipped with nine thin film heat flux gages that provide simultaneous heat flux and temperature measurements. The

septum plate is instrumented with 23 metal-sheathed Type K thermocouples, and is heated by the radiant heater array. The 304.8 × 304.8 mm Q-fiber test sample was placed between the water-cooled and septum plates having the same planar area. For these tests, no picture frames or spacers were utilized between the water-cooled and septum plates, and the septum plate was placed directly on top of the test specimen. The effective thickness of the test specimen after being compressed by the weight of the septum plate was measured to be 19.05 mm. The resulting density of the insulation test specimen was 68.8 kg/m^3. The calculated effective thermal conductivities at the four heat flux gage locations in the central 127 × 127 mm section of the test setup were used to provide the average effective thermal conductivity [19].

The average overall uncertainty of the effective thermal conductivity measurements over the range of pressures and temperatures in the LaRC thermal-vacuum testing apparatus had been previously determined to be 7.5% [19], with higher uncertainties at the lowest pressures and temperatures. A detailed uncertainty analysis [22] was conducted in the present study for each measured quantity: hot and cold side temperatures, heat fluxes, and for the calculated effective thermal conductivities. The overall uncertainty consisted of the contributions of random and bias uncertainties for each measured quantity, and uncertainties due to spatial non-uniformity of averaged quantities [23].

Tests were conducted with nominal septum plate temperatures of 366, 533, 698, 864, 1030, 1140, 1252, and 1360 K. The water-cooled plate was maintained around room temperature. At each hot side temperature set point, tests were conducted at nominal environmental pressures of 0.001, 0.01, 0.1, 1, 10, 100, and 750 torr. All the measurements were conducted in a gaseous nitrogen environment. The average water-cooled plate temperature for the data reported in this study was 300.8 ± 3.6 K.

ANALYTICAL APPROACH

The theoretical expression for the total thermal conductivity of Q-fiber, assuming optically thick radiation, will be provided, which consists of contributions of radiation, solid and gaseous conduction. Unlike the lumped thermal conductivity, the total thermal conductivity model can be used to calculate the thermal conductivity of insulation as a function of local temperature and pressure for any set of composition parameters, such as various densities. For model verification purposes the calculated total thermal conductivity needs to be integrated over the range of experimental hot and cold side temperatures for comparison with measured effective thermal conductivity (measured over a large temperature gradient).

Radiation Model

A brief description of the radiation model is provided, with the details provided in the literature [4]. Using the diffusion approximation for the optically thick case, radiation heat transfer can be expressed in terms of a radiation conductivity, k_r, similar to the Fourier's law of heat conduction

$$q_r = k_r \frac{dT}{dy} \tag{1}$$

The radiative conductivity is calculated using the modified Rosseland absorption coefficient that accounts for the two-dimensional scattering characteristics of fibers

$$k_r = \frac{16\sigma n^2 T^3}{3} \int_0^\infty \frac{1}{\Gamma_\lambda} \frac{dI_{b\lambda}(T)}{dI_b(T)} d\lambda \tag{2}$$

where σ is the Stefan-Boltzmann constant, n is the index of refraction, and I is the radiant intensity. The modified absorption coefficient, Γ_λ, is given by

$$\Gamma_\lambda = K_\lambda(\mu_0)(1 - G_\lambda) \tag{3}$$

where K_λ is the extinction coefficient of the fiber medium in the heat flow direction $(\mu_0 = cos\xi_0)$, ξ the polar angle, and G_λ the asymmetrical scattering factor which is derived from the product of the scattering coefficient and the phase function. As typical unbonded fibrous media have a range of fiber diameters and orientations, the spectral extinction and scattering coefficients are obtained by weighting the cross sections over the distribution of sizes and orientations. Details on the calculation of the scattering factor and extinction coefficient are provided elsewhere [4, 15, 16]. Q-fiber size distribution was obtained from microscopic data and orientation was assumed to be random in space. Mean diameter was 1.53×10^{-6} m and an equivalent diameter for radiation based on the distribution of diameters was 2.88×10^{-6} m.

Solid Conduction Model

The semi-empirical approach used to model solid conduction in the fibrous insulation was [4]

$$k_c(T) = F_s \rho_s^b k_s(T) \tag{4}$$

where ρ_s is the density of the fiber matrix, and k_s is the thermal conductivity of the bulk material. The model assumes that the solid conductivity is independent of fiber diameter and varies with density raised to a power [3, 18]. The exponent b is typically between 1 and 2. The parameter F_s is a global property that relates the micro-scale geometric effects of fiber matrix with bulk dimensions, and accounts for the various fiber path lengths, fiber arrangement, and fiber to fiber contacts. F_s is assumed to be temperature independent and is typically obtained from guarded hot plate thermal conductivity measurements in vacuum at cryogenic temperatures (test condition with negligible radiation and gas conduction).

Gas Conduction Model

The thermal conductivity associated with gas conduction in the void space of high porosity fibrous insulations is a function of the pore size and the gas mean free path [3]

$$k_g(T,P) = \frac{k_{g0}(T)}{1 + \frac{2\beta}{Pr}\frac{\lambda}{L_c}} \qquad (5)$$

where $k_{g0}(T)$ is the pressure-independent thermal conductivity of the gas, and Pr is the Prandtl number. The parameter β is defined as

$$\beta = (\frac{2-\alpha}{\alpha})\frac{2\gamma}{(\gamma+1)} \qquad (6)$$

with α being the thermal accommodation coefficient, and γ being the ratio of specific heats at constant volume and pressure. The gas mean free path, λ, is

$$\lambda = \frac{K_B T}{\sqrt{2}\pi d_m^2 P} \qquad (7)$$

where K_B the Boltzmann constant, d_m the gas collision diameter, and P the pressure. Determination of gas conduction characteristic length, pore diameter, in fibrous insulation mats is not trivial. A semi-empirical formulation for characteristic length, L_c, is used [3]

$$L_c = \zeta \frac{d_p}{f} \qquad (8)$$

where f is the solid volume fraction of the fibers, and d_p the fiber mean diameter. The constant ξ is either 0.524 for fibers randomly oriented in space [24], or 0.785 for fibers randomly oriented in planes [3]. The former was used in this study. A comparison between experimental measurements of pore diameters and calculated values for fibrous materials is given by Kagner [25]. Typically, the experimental values are 1.5 to 2.0 times those calculated from theory. The equivalent radiation fiber diameter of 2.88×10^{-6} m was used for d_p.

Total Thermal Conductivity

The total thermal conductivity is then obtained by superposition of the thermal conductivities due to radiation, solid conduction, and gas conduction from Eqs. (2), (4), and (5)

$$k = k_r + k_c + k_g \qquad (9)$$

In order to compare the theoretical predictions with experimental measurements, the total thermal conductivity predicted using Eq. (9) had to be numerically integrated with respect to temperature between the experimental hot and cold side temperatures, T_H and T_C

$$k_e = \frac{1}{T_H - T_C}\int_{T_C}^{T_H} k\partial T \qquad (10)$$

DISCUSSION OF RESULTS

The comparison of measured and predicted effective thermal conductivities as a function of the hot side temperature, T_H, at pressures of 0.001, 1, and 100 torr is shown in Figure 2a, while the data at pressures of 0.1, 10, and 750 torr is provided in Figure 2b. The error bars correspond to experimental uncertainties at each individual data point. The experimental uncertainties are highest at the lowest test temperatures and pressures, where the heat flux levels are too low for the resolution of the heat flux gages used, and decrease with increasing pressure and temperature. For hot side temperatures of 533, 864, and 1360 K, the experimental uncertainties varied between 29 and 5%, 2.4 and 2.2%, and 3.3 and 1.7%, respectively, with the highest and lowest uncertainties corresponding to pressures of 0.001 and 750 torr, respectively. The uncertainties of the predicted effective thermal conductivities due to uncertainties in optical properties and fiber size are of the order of 8 to 12% [4]. At a pressure of 0.001 torr solid conduction and radiation are the only modes of heat transfer, with radiation being the dominant mode, especially as temperature increases. The close agreement between the predicted and measured effective thermal conductivity data at 0.001 torr verifies the radiation modeling developed by Lee and Cunnington [4]. The difference between measured and predicted thermal conductivities at this pressure varies between 1 and 4% for T_H between 700 and 1360 K. The difference is larger at lower temperatures (32 and 24% at T_H of 363 and 533, respectively) due to the large uncertainty in the experimental data at low heat fluxes.
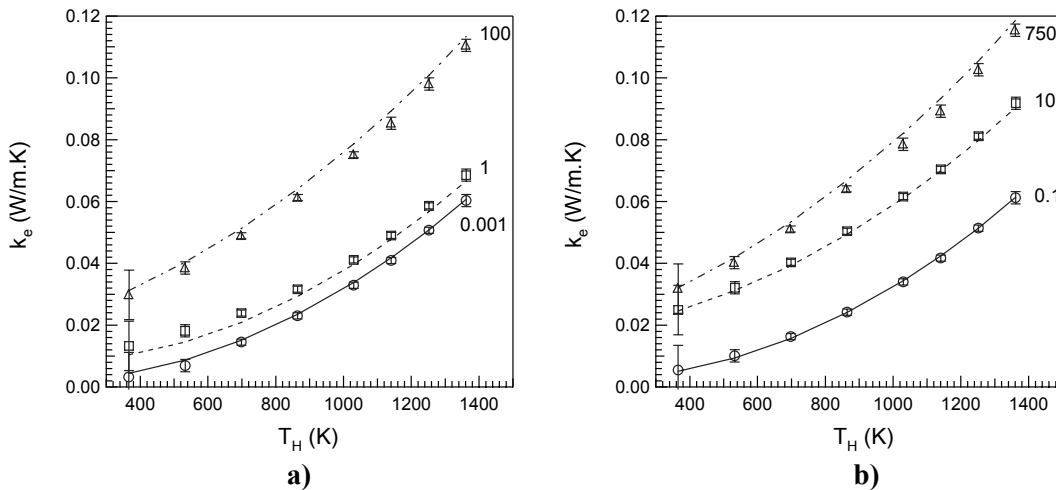

Figure 2. Comparison of measured and predicted effective thermal conductivities for Q-fiber at a density of 68.8 kg/m^3 at various pressures: a) 0.001, 1, and 100 torr,
b) 0.1, 10, 750 torr

There is close overall agreement between measured and predicted effective thermal conductivities at all pressures and at hot side temperatures equal to or greater than 533 K. The root mean square (rms) difference between measurements and predictions for all the measured data points with $T_H \geq 533$ K is 5.9%. . The

close agreement between predictions and measurements over the entire pressure range of 0.001 to 750 torr further verifies the overall heat transfer model.

The combined radiation/conduction model was also applied to an earlier set of data generated using the same apparatus on 13.3 mm thick Q-fiber samples at densities of 48.6 and 95.6 kg/m^3 [19]. For these tests, data had been generated at nominal hot side temperatures of 366, 533, 695, 862, 1028, 1140, and 1251 K, and at nominal pressures of 0.0001, 0.001, 0.01, 0.1, 0.5, 1, 5, 10, 100, and 750 torr. Comparison of measured and predicted effective thermal conductivities as a function of hot side temperature for pressures of 0.001, 1, and 100 torr for sample densities of 48.6 and 95.6 kg/m^3 are shown in Figures 3a and 3b, respectively. Detailed experimental uncertainty data for each individual data point was not available for these data sets, therefore the overall average experimental uncertainty of 7.5% [19] was used in the figures. There is close agreement between the measured and predicted thermal conductivities as shown in the figures. The rms differences between predicted and measured effective thermal conductivities for the entire set of data with $T_H \geq 533$ K were 6.1 and 10.5% for the sample densities of 48.6 and 95.6 kg/m^3, respectively.
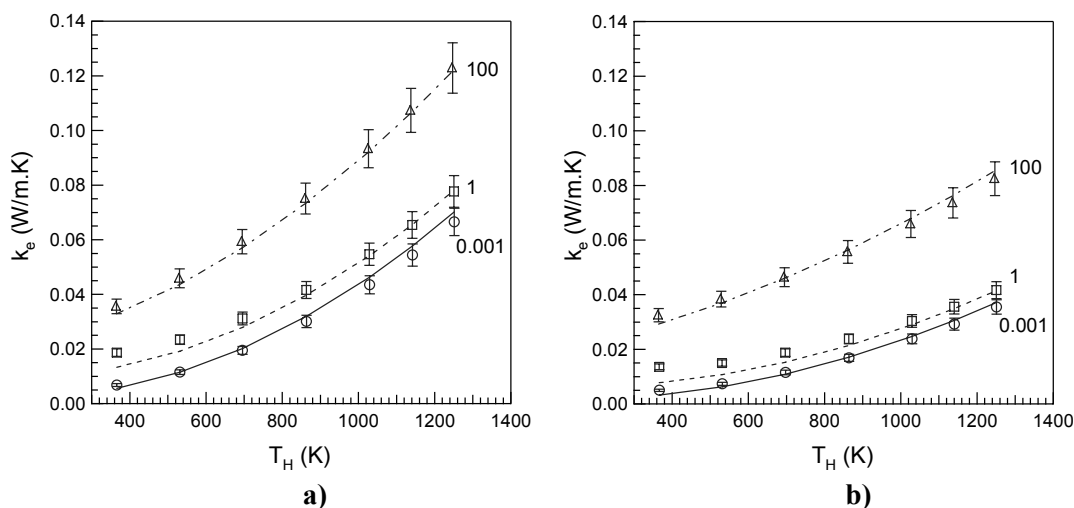

Figure 3. Comparison of measured and predicted effective thermal conductivities for Q-fiber
at pressures of 0.001, 1, and 100 torr, for densities of
a) 48.6 kg/m^3 ; b) 95.6 kg/m^3

The close agreement between measured and predicted effective thermal conductivities over the pressure range of 0.0001 to 750 torr, and hot side temperature range of 533 to 1360 K, for three Q-fiber samples at densities of 48.6, 68.8, and 95.6 kg/m^3 further validates the previously developed combined radiation/ conduction model [4] for formulating heat transfer in high-porosity unbonded fibrous insulation samples. The radiation model includes a rigorous formulation for scattering properties of fibrous insulations that accounts for the fiber orientation in the medium, with the radiative properties as a function of orientation, size distribution and volume fraction of fibers.

CONCLUDING REMARKS

Effective thermal conductivity of a high porosity unbonded silica fibrous insulation specimen (Q-fiber) at a density of 68.8 kg/m^3 was measured over a pressure range of 0.001 to 750 torr and a temperature range of 360 to 1360 K. Measurements were performed with large temperature gradients maintained across the sample. The measurements were compared with the solution of combined radiation/conduction heat transfer. The previously developed radiation heat transfer model [4] used in this study is based on a modified diffusion approximation, and uses deterministic parameters that define the composition and morphology of the medium: distributions of fiber size and orientation, fiber volume fractions, and the spectral complex refractive index of the fibers The theoretical model was also applied to previously reported data on Q-fiber at densities of 48.6, and 95.6 kg/m^3, generated using the same experimental technique. Ignoring data at the lowest hot side temperature (T_H = 366 K), the rms differences between measured and predicted effective thermal conductivities were 6.1, 5.9, and 10.5% for sample densities of 48.6, 68.8, and 95.6 kg/m^3, respectively. The uncertainties of the predicted effective thermal conductivities due to uncertainties in optical properties and fiber size are of the order of 8 to 12%, while the corresponding experimental uncertainties varied between 1.2 and 29%. The close agreement between experimental and theoretical data further validates the theoretical approach over a wide range of temperatures and pressures.

REFERENCES

1. Stark, C., and Fricke, J., "Improved Heat-Transfer Models for Fibrous Insulations," *International Journal of Heat and Mass Transfer*, Vol. 36, No. 3, 1993, pp. 617-625.

2. Daryabeigi, K., "Heat Transfer in High-Temperature Fibrous Insulation," *Journal of Thermophysics and Heat Transfer*, Vol. 17, No. 1, pp.10-20, 2003.

3. Verschoor, J. D., and Greebler, P., and Manville, N.J., "Heat Transfer by Gas Conduction and Radiation in Fibrous Insulations," *Transactions of the Society of Mechanical Engineers*, Vol. 74, No. 8, 1952, pp. 961-968.

4. Lee, S. C., and Cunnington, G. R., "Conduction and Radiation Heat Transfer in High-Porosity Fiber Thermal Insulation," *Journal of Thermophysics and Heat Transfer*, Vol. 14, No. 2, 2000, pp. 121-136.

5. Gebhart, B., *Heat Conduction and Mass Diffusion*, McGraw-Hill, New York, 1993, pp. 442-444.

6. Lee, S. C., and Cunnington, G. R, "Theoretical Models for Radiative Transfer in Fibrous Media," *Annual Review in Heat Transfer*, ed. By C. L. Tien, Vol. 9, Begell House, NY, 1998, pp. 641-646.

7. Banas, R.P, and Cunnington, G. R., "Determination of Effective Thermal Conductivity for the Space Shuttle Orbiter's Reusable Surface Insulation," AIAA 74-730, July 1974.

8. Williams, S. D., and Curry, D. M., "Predictions of Rigid Silica Based Insulation Conductivity," NASA TP-3276, January 1993.

9. Stewart, D. A. and Leiser, D. B., "Characterization of the Thermal Conductivity for Advanced Toughened Uni-piece Fibrous Insulation," AIAA 93-2755. July 1993.

10. Yuen, W. W., and Cunnington, G. R., "Heat Transfer Characteristics of High Porosity Fibrous Insulation Materials (Analysis of Radiative Heat Transfer Using the Zonal-GFE Method)," AIAA 2005-192, January 2005.

11. Roux, J. A., Smith, A.M., "Combined Conduction and Radiation Heat Transfer in a Absorbing and Scattering Medium," American Inst. of Chemical Engineers/American Society of Mechanical Engineers, Paper HT-50, Aug. 1977.

12. Matthews, L. K., Viskanta, R., and Incropera, F. P., "Combined Conduction and Radiation Heat Transfer in Porous Materials Heated by Intense Solar Radiation," *Journal of Solar Energy Engineering*, Vol. 107, February 1985, pp. 29-34.

13. Tong, T. W., and Tien, C. L., "Radiative Heat Transfer in Fibrous Insulations-Part I: Analytical Study," *Journal of Heat Transfer*, Vol. 105, February 1983, pp. 70-75.

14. Tong, T. W., Yang, Q. S., and Tien, C. L., "Radiative Heat Transfer in Fibrous Insulations-Part II: Experimental Study," *Journal of Heat Transfer*, Vol. 105, February 1983, pp. 76-81.

15. Lee, S. C., "Radiative Transfer Through a Fibrous Medium: Allowance for Fiber Orientation," *Journal of Quantitative Spectroscopy and Radiative Transfer*, Vol. 36, No. 3, 1986, pp. 253-263.

16. Lee, S. C., "Scattering Phase Function for Fibrous Materials," *International Journal of Heat and Mass Transfer*, Vol. 33, No. 10, 1990, pp. 2183-2190.

17. ASTM Standard C 177, "Standard Test Method for Steady-State Heat Flux Measurements and Thermal Transmission Properties by Means of the Guarded-Hot-Plate Apparatus," Annual Book of ASTM Standards, Vol. 4.06, *Thermal Insulation, Environmental Acoustics*, 1996.

18. Pettyjohn, R. R., "Thermal Conductivity Measurements on a Fibrous Insulation Material," *Proceedings of the Seventh Conference on Thermal Conductivity*, NBS Special Publication 302, edited by D. R. Flynn and B. A. Leavy Jr., U.S. Government Printing Office, Washington, DC, 1968, pp 729-736.

19. Daryabeigi, K., "Effective Thermal Conductivity of High Temperature Insulations for Reusable Launch Vehicles," NASA TM-1999-208972, February 1999.

20. Daryabeigi, K., "Analysis and Testing of High Temperature Fibrous Insulation for Reusable Launch Vehicles," AIAA Paper 99-1044, January 1999.

21. Standard Test Method for Thermal Conductivity of Refractories, *Annual Book of ASTM Standards,* Vol. 15.01, American Society for Testing and Materials, West Conshohocken, PA, pp. 54-59, 2000.

22. Coleman, H. W., and Steele, W. G., *Experimentation and Uncertainty Analysis for Engineers*, Wiley, New York, 1989.

23. Sullins, A. D., "Heat Transfer in High Porosity Open Cell Nickel Foam," M.S. Thesis, School of Engineering and Applied Sciences, The George Washington University, August 2001.

24. Keller, K., Blumenberg, J., and Tomsik, J., "Fibre Orientation and the Conduction of Heat by a Gas Enclosed in Ceramic Layers," *ZFW*, Vol. 12, 1988, pp. 258-260.

25. Kagner, M. G., *Thermal Insulation in Cryogenic Engineering*, Israel Program for Scientific Translations, Jerusalem, 1969, Chapter IV, pp. 75-76.